

**Basic chemokine-derived glycosaminoglycan binding peptides exert antiviral properties against dengue virus serotype 2, herpes simplex virus-1 and respiratory syncytial virus**

Vincent Vanheule<sup>a,c</sup>, Peter Vervaeke<sup>b,c</sup>, Anneleen Mortier<sup>a</sup>, Sam Noppen<sup>b</sup>, Mieke Gouwy<sup>a</sup>, Robert Snoeck<sup>b</sup>, Graciela Andrei<sup>b</sup>, Jo Van Damme<sup>a</sup>, Sandra Liekens<sup>b,d</sup>, Paul Proost<sup>a,d</sup>

<sup>a</sup> KU Leuven - University of Leuven, Department of Microbiology and Immunology, Rega Institute for Medical Research, Laboratory of Molecular Immunology, B-3000 Leuven, Belgium

<sup>b</sup> KU Leuven - University of Leuven, Department of Microbiology and Immunology, Rega Institute for Medical Research, Laboratory of Virology and Chemotherapy, B-3000 Leuven, Belgium

<sup>c</sup> V. Vanheule and P. Vervaeke: equally contributed first authors

<sup>d</sup> P. Proost and S. Liekens: equally contributed senior authors

E-mail addresses:

vincent.vanheule@rega.kuleuven.be; peter.vervaeke@rega.kuleuven.be;

anneleen.mortier@rega.kuleuven.be; sam.noppen@rega.kuleuven.be;

mieke.gouwy@rega.kuleuven.be; robert.snoeck@rega.kuleuven.be;

graciela.andrei@rega.kuleuven.be; jo.vandamme@rega.kuleuven.be;

sandra.liekens@rega.kuleuven.be; paul.proost@rega.kuleuven.be

Corresponding author: Paul Proost, Laboratory of Molecular Immunology, Rega Institute for Medical Research, KU Leuven, Minderbroedersstraat 10, B-3000 Leuven, Belgium

Email: paul.proost@rega.kuleuven.be; Tel.: +32-16-337341; Fax.: +32-16-337340

## ***Abstract***

Chemokines attract leukocytes to sites of infection in a G protein-coupled receptor (GPCR) and glycosaminoglycan (GAG) dependent manner. Therefore, chemokines are crucial molecules for proper functioning of our antimicrobial defense mechanisms. In addition, some chemokines have GPCR-independent defensin-like antimicrobial activities against bacteria and fungi. Recently, high affinity for GAGs has been reported for the positively charged COOH-terminal region of the chemokine CXCL9. In addition to CXCL9, also CXCL12 $\gamma$  has such a positively charged COOH-terminal region with about 50 % positively charged amino acids. In this report, we compared the affinity of COOH-terminal peptides of CXCL9 and CXCL12 $\gamma$  for GAGs and  $K_D$  values in the low nM range were detected. Several enveloped viruses such as herpesviruses, hepatitis viruses, human immunodeficiency virus (HIV), dengue virus (DENV), etc. are known to bind to GAGs such as the negatively charged heparan sulfate (HS). In this way GAGs are important for the initial contacts between viruses and host cells and for the infection of the cell. Thus, inhibiting the virus-cell interactions, by blocking GAG-binding sites on the host cell, might be a way to target multiple virus families and resistant strains. This article reports that the COOH-terminal peptides of CXCL9 and CXCL12 $\gamma$  have antiviral activity against DENV serotype 2, clinical and laboratory strains of herpes simplex virus (HSV)-1 and respiratory syncytial virus (RSV). Moreover, we show that CXCL9(74-103) competes with DENV envelope protein domain III for binding to heparin. These short chemokine-derived peptides may be lead molecules for the development of novel antiviral agents.

## ***Keywords***

chemokine; glycosaminoglycan; antiviral activity; dengue virus; heparan sulfate

## **1. Introduction**

The emergence of drug-resistant viruses and the absence of vaccination strategies for several viruses evokes the need for novel classes of antivirals [1;2]. Previously, antiviral drugs targeting the binding and entry of viruses such as human immunodeficiency virus (HIV), hepatitis C virus (HCV) and herpes simplex viruses type 1 and 2 (HSV-1 and -2) were developed and approved or are currently undergoing clinical trials [3-5]. Blocking the viral infection at this early stage is less toxic with less side effects compared to chemotherapeutics affecting the viral multiplication cycle that are currently used. Examples of binding and entry inhibitors are maraviroc [6;7], a chemokine receptor antagonist preventing the entry of HIV, and carbohydrate-binding agents that bind to glycoproteins on the virus surface thereby preventing infection with dengue virus (DENV) [8]. DENV is one of the most important emerging viruses in tropical and subtropical countries with 2.5 billion people at risk to get infected and every year more than 50 million clinical cases of DENV infections [9]. Further, it was shown that several viruses such as HSV-1, hepatitis B virus (HBV), HIV-1, DENV, vaccinia virus (VV) and adenovirus (ADV) bind to glycosaminoglycans (GAGs) for entering and infecting the host cell [10-19]. GAGs are linear polysaccharides consisting of repeating disaccharide subunits which can be divided into six classes: heparin, heparan sulfate (HS), chondroitin sulfate, dermatan sulfate, keratan sulfate and hyaluronic acid [20]. Several interactions of GAGs with proteins have already been described for growth factors (e.g. fibroblast growth factor-1 and -2), adhesion molecules, enzymes and chemokines (e.g. CXCL8 and CXCL4) [21;22]. As a result of these interactions, GAGs participate in many physiological and pathological processes such as cell growth, signal transduction, cell adhesion, inflammation, cancer and microbial infection [23-25]. HS, consisting of alternating glucosamine and uronic acids residues that can be N-acetylated or N-sulfated, is ubiquitously present on most mammalian cells and tissues and is expressed as heparan sulfate proteoglycans (HSPGs) whereby GAGs are covalently attached to a central core protein. Because of its high degree of sulfation, HS contains a considerable number of negatively charged groups which can interact with viral proteins that carry positive charges. In this way HS is important for the initial contacts between viruses and host cells. However, not only the

nonspecific ionic interactions are important for the binding of viruses to HS, this binding is suggested to be more complex in several ways. First, it has been suggested that cell surface HS could serve as a specific binding site for several viruses such as DENV, HSV-1 and HIV-1 [12;26-28]. Second, saccharide structures of HS have different activities in promoting viral infections. For example, for the binding of HSV-1 to cells, highly sulfated HS interacts with viral glycoproteins C and B [29;30]. Subsequently, specific 3-O-sulfated HS interacts with viral glycoprotein D which is essential for entry of the virus [26;31].

Although it has already been shown that suramin, a substance that inhibits binding to HS on the membrane of hepatocytes, blocks entry of HBV, hepatitis D virus (HDV) and HIV *in vitro*, no antiviral drugs targeting this interaction have yet been developed [32]. However, more recently, a new class of synthetic peptides with a sequence based on the lipopolysaccharide (LPS)-binding domain of the Limulus anti-LPS factor was shown to block attachment and entry of human pathogenic viruses [33]. These synthetic anti-LPS peptides bind to HS on the cell surface of the host cells and inhibit infection with a variety of enveloped viruses such as HIV-1, HSV-1 and HSV-2, HBV and HCV. In addition, novel HS-binding peptides that block entry of herpesviruses were synthesized [34]. Thus, inhibiting the virus-cell interactions, by blocking GAG binding sites on the host cell, is a way to target multiple virus types and resistant virus strains.

Chemokines are a class of leukocyte chemotactic cytokines which exert their function through binding both to GAGs and to G protein-coupled receptors (GPCRs) and GAG binding is indispensable for the *in vivo* function of chemokines [35-42]. Chemokines can be divided into four groups based on the position of two conserved NH<sub>2</sub>-terminal cysteine residues. The CC chemokines have two adjacent cysteine residues, whereas in CXC and CX<sub>3</sub>C chemokines these residues are separated by one or three amino acids (X), respectively [43]. In the C chemokine subfamily only one of the two NH<sub>2</sub>-terminal cysteine residues is conserved. Recently, COOH-terminal peptides of the chemokine CXCL9 or monokine induced by interferon- $\gamma$  (MIG) were described as potent GAG binding peptides [44]. By

competing with CXCL8 for the binding to GAGs, these peptides could inhibit the *in vivo* chemotactic activity of CXCL8. These peptides could not only inhibit CXCL8-induced neutrophil extravasation but also monosodium urate crystal-induced gout in mice. This implies that *in vivo* not only the activity of CXCL8, but the activity of multiple mouse chemotactic factors important in monosodium urate crystal-induced gout could be inhibited. In addition to CXCL9, also CXCL12 $\gamma$  or stromal cell-derived factor-1 $\gamma$  (SDF-1 $\gamma$ ) has a COOH-terminal region with many positively charged amino acids [45]. Therefore, the GAG binding affinity of COOH-terminal peptides of CXCL9 and CXCL12 $\gamma$ , which are remarkably long and basic with 50 % of the amino acids being positively charged, were compared in this study and their potential to inhibit infection of cells with several viruses such as DENV, HSV-1, HSV-2 and respiratory syncytial virus (RSV) was evaluated.

## **2. Materials and Methods**

### *2.1. Cells and viruses*

Chinese hamster ovary (CHO) cells were a gift from M. Parmentier (ULB, Brussels, Belgium) and were cultured in Ham's F-12 medium (with L-glutamine; Lonza, Verviers, Belgium) supplemented with 10 % fetal calf serum (FCS) and 0.8  $\mu$ g/ml G418 (Geneticin<sup>®</sup>; Life technologies). To inhibit sulfation of cellular GAGs, CHO cells were cultured in the presence of 100 mM sodium chlorate (NaClO<sub>3</sub>; Sigma Aldrich, St. Louis, MO) for 24 h [44]. Human embryonic lung (HEL) and human cervical carcinoma (HeLa) cells were grown in modified Eagle's medium Rega 3 supplemented with 8 % FCS, 2 mM L-glutamine and 1.5 % sodium bicarbonate (Gibco, Carlsbad, CA, USA). The human microvascular endothelial cell line HMEC-1 was obtained from the Centers for Disease Control and Prevention (CDC, Atlanta, GA, USA) and was grown in microvascular endothelial cell growth medium (Lonza) [46]. All cell types were maintained in a humidified 5 % CO<sub>2</sub> incubator at 37°C.

The peptides were tested against the following viruses: HSV-1 KOS strain, HSV-2 G strain, VV Lederle strain, ADV type 2 (ADV-2), RSV, and DENV serotype 2 (DENV-2). Also several clinical isolates of wild-type HSV-1 (RV-852, RV-849, RV-832, RV-830) and wild-type HSV-2 (RV-795, RV-723, RV-720, RV-636)

from virus-infected individuals in Belgium were used. All viruses were obtained and used approved by the Belgian equivalent of IRB (Departement Leefmilieu, Natuur en Energie, protocol SBB 219 2011/0011) and the Biosafety Committee at KU Leuven. Antiviral assays were performed in infection medium, i.e. modified Eagle's medium Rega 3 supplemented with 2 % FCS, 2 mM L-glutamine and 1.5 % sodium bicarbonate for HEL and HeLa cells, and microvascular endothelial cell growth medium for HMEC-1 cells.

## *2.2. Solid phase synthesis of COOH-terminal peptides*

COOH-terminal peptides of CXCL9 and CXCL12 $\gamma$  were chemically synthesized using fluorenyl methoxycarbonyl (Fmoc) chemistry using an Activo-P11 automated synthesizer (Activotec, Cambridge, UK), as previously described [47]. In brief, peptides were synthesized based on solid-phase synthesis conducting cycles of (1) deprotection, (2) activation and (3) coupling. The  $\alpha$ -carboxyl group of the COOH-terminal amino acid was attached to a solid support, namely HMP-resin (4-hydroxymethylphenoxy-methyl-polystyrene, cross-linked by 1 % divinylbenzene). After each coupling step the remaining free  $\alpha$ -amino acids were capped. Part of the material was site-specifically biotinylated or fluorescently labeled at the NH<sub>2</sub>-terminus using biotin-p-nitrophenyl ester (Novabiochem, Darmstadt, Germany) or 5(6)-carboxytetramethylrhodamine (TAMRA; Merck Millipore, Darmstadt, Germany) applying the standard amino acid coupling chemistry. After removal of the resin beads and side chain protection groups, intact synthetic peptides were separated from incompletely synthesized by-products by reversed-phase high performance liquid chromatography (RP-HPLC) on a Source 5-RPC column (4.6 x 150 mm; GE Healthcare, Little Chalfont, UK) applying an acetonitrile gradient in 0.1 % (v/v) trifluoroacetic acid (Biosolve, Valkenswaard, The Netherlands). A part of the column effluent (0.7 %) was split for analysis to an Amazon SL ion trap mass spectrometer (Bruker, Bremen, Germany) and fractions containing pure peptide were pooled and lyophilized. To determine the protein concentration, the weight of the dry peptide powder was measured on an analytical scale before dissolving it in ultrapure water.

### *2.3. Binding of COOH-terminal peptides to cellular GAGs and competition with CXCL8*

Binding of biotinylated peptides to CHO cells was assessed by flow cytometry as recently described [48]. Briefly, cells were detached by phosphate-buffered saline (PBS) containing 0.02 % ethylenediaminetetraacetic acid (EDTA; Sigma Aldrich). Subsequently,  $2.5 \times 10^5$  cells were incubated with NH<sub>2</sub>-terminally biotinylated peptides for 1 h on ice, washed and incubated for 30 min on ice in the dark with streptavidin-allophycocyanin [1/150; BD Biosciences, San Jose, CA]. Finally, cells were washed with ice-cold assay buffer, fixed and analyzed by flow cytometry (FACSCalibur, BD Biosciences).

### *2.4. Flow cytometric analysis of HS expression*

To confirm inhibition of sulfation of cellular GAGs after NaClO<sub>3</sub> treatment, part of the CHO cells were stained with a mouse monoclonal anti-human HS antibody (Immunosource, Schilde, Belgium), washed, incubated with a secondary phycoerythrin-labeled goat anti-mouse antibody (1/150; BD Biosciences) and analyzed by flow cytometry. HEL and Hela cells were stained and analyzed in a similar way. Statistical analyses were performed using the Mann-Whitney U-test.

### *2.5. Biotinylation of heparin and surface plasmon resonance (SPR) analysis*

1 mM of heparin (Sigma Aldrich) and 10 mM biotinamidohehexanoic acid hydrazide (Sigma Aldrich) were mixed in PBS at room temperature for 24 h. Afterwards, the mixture was dialyzed against PBS to remove unreacted biotin.

SPR was used to evaluate binding between synthetic CXCL9- and CXCL12 $\gamma$ -derived peptides and heparin. Neutravidin (Perbio science bvba, Erembodegem, Belgium) was covalently immobilized on two flow cells of a Series S Sensor Chip CM4 in 10 mM sodium acetate, pH 5.5, using standard amine coupling chemistry, resulting in chip densities of 2000 RU. Next, biotinylated heparin was captured on the second flow cell at 76 RU. The first flow cell was left untreated and was used as a control for non-specific binding and refractive index changes. All interactions were performed at 24 °C on a Biacore T200 instrument (GE Healthcare, Uppsala, Sweden) in HBS-EP (10 mM HEPES, 150 mM NaCl, 3 mM

EDTA and 0.05 % surfactant P20; pH 7.4). Samples were injected for 2 min at a flow rate of 30  $\mu$ l/min and the dissociation phase was followed for 5 min. Several buffer blanks were used for double referencing. The second sensor chip surface was regenerated with 1 M NaCl (30 sec) and stabilized for another 5 min. Binding affinities ( $K_D$ ) were derived from steady state analysis using the Biacore T200 Evaluation Software 2.0. To evaluate competition between recombinant envelope (E) protein domain III of DENV-2 and the synthetic peptides for heparin binding the same sensor chip was used. The analytes, 400 nM of E protein domain III alone or premixed with a concentration range of the synthetic CXCL9- or CXCL12 $\gamma$ -derived peptides were injected for 2 min at a flow rate of 30  $\mu$ l/min, followed by a dissociation phase of 2 min. The sensor chip surface was regenerated with 10 mM NaOH containing 1 M NaCl.

#### *2.6. Antiviral and cytotoxicity assays*

HeLa and HEL cells were seeded in microtiter 96-well plates and grown to confluence. Confluent monolayers were inoculated with 100 CCID<sub>50</sub> of virus (50 % cell culture infectious dose, 1 CCID<sub>50</sub> being the amount of virus that infects 50 % of the cell culture) in the presence of serial dilutions of the synthetic peptides [49-51]. The antiviral activity was determined by the ability to inhibit the virus-induced cytopathogenic effect in the different cell lines (HeLa cells for infection with RSV and HEL cells for infection with HSV-1, HSV-2, ADV-2 and VV). In addition, to investigate whether the peptide binds directly to the virus, HSV-1 (100x) was incubated with 100  $\mu$ M CXCL9(74-103) for 30 min. Next, the mixture was diluted 100-fold to obtain an inactive peptide concentration and an active virus concentration and added to HEL cells. Viral cytopathogenicity was determined when it reached 100 % in the untreated cell control and antiviral activity was expressed as the EC<sub>50</sub> value (effective concentration of peptide required to reduce virus-induced cytopathogenicity by 50 %). Inhibition of DENV-2 infection of HMEC-1 cells was evaluated in gelatin-coated 48-well plates. After an overnight incubation, confluent monolayers were infected with DENV-2 at a multiplicity of infection of 2 plaque forming units in the presence of different concentrations of the peptides. Cells were analyzed for DENV



infection by flow cytometry at 24 h after infection, as described previously [52]. The EC<sub>50</sub> value was determined as the peptide concentration required to inhibit DENV-2 infection of HMEC-1 cells by 50 %.

Potential cytotoxic effects of the compounds were evaluated in parallel by 3-(4,5-dimethylthiazol-2-yl)-5-(3-carboxymethoxyphenyl)-2-(4-sulfophenyl)-2H-tetrazolium method (MTS; Promega Corporation, Madison, WI). HeLa and HEL cells were seeded in 96-well plates and grown to confluence. Confluent monolayers were incubated with serial dilutions of the synthetic peptides. Next, medium was replaced by 100 µl of 0.02 % MTS in PBS and incubated for 2 h at 37 °C. The optical density was determined at 490 nm and the 50 % cytotoxic concentration (CC<sub>50</sub>; i.e. drug concentration needed to reduce the total cell number by 50 %) was calculated.

### *2.7. Induction experiments and cytokine levels*

For the induction experiments, cells were seeded in microtiter 48-well plates and grown to confluence. Confluent monolayers were inoculated with RSV, HSV-1 or DENV-2, as described above, in the presence or absence of the synthetic peptides (25 µM). Furthermore, confluent monolayers were incubated with vehicle or peptides alone. Supernatants were collected after 24 h and after 4 days for, respectively, infection with DENV-2 and infection with RSV or HSV-1 and kept at -20 °C for further use. The cytokine levels of interleukin-6 (IL-6), tumor necrosis factor-α (TNF-α), interleukin-1β (IL-1β), interferon-α (IFN-α) and interferon-β (IFN-β) in the supernatants were measured using ELISA kits according to the manufacturer's instructions. Human IL-1β, TNF-α and IL-6 were measured by a DuoSet® sandwich ELISA (DuoSet® ELISA Development System, R&D Systems, Minneapolis, USA) and human IFN-α and IFN-β were measured by VeriKine-HS Human Interferon α or β Serum ELISA Kits (PBL Assay Science, NJ, USA).

### *2.8. Caspase-1 activity assay*

Cells from induction experiments were lysed with buffer containing 20 mM HEPES, 100 mM NaCl, 10 mM dithiothreitol (DTT), 100 µM phenylmethylsulfonyl fluoride (PMSF), 1 mM EDTA, 0.1 % CHAPS, 10 % sucrose and 1 % Triton-X-100 (pH 7.2). The protein concentration of each sample was determined and equal amounts of lysate were incubated with 50 µM of acetyl-Tyr-Val-Ala-Asp-

aminomethylcoumarin (Ac-YVAD-AMC; Enzo Life Sciences, Antwerp, Belgium) in 100 mM Tris (pH 7.2) at 37 °C. Fluorescence of the free AMC fluorophore was measured for 4-10 h at 10-min intervals by fluorometry (excitation and emission wavelengths of 340-360 nm and 440-460 nm).

### *2.9. Immunocytochemistry*

HMEC-1 cells were seeded on gelatin-coated 8-well Millicell EZ slides (Merck Millipore). Confluent monolayers were infected with DENV-2 as described above in the presence or absence of 20 µM of TAMRA-labeled CXCL9(74-103). After 24h the cells were fixed in 2% paraformaldehyde and permeabilized with 0.1% Triton X-100. Nonspecific binding sites were blocked with 0.5% bovine serum albumin in PBS. The cells were incubated with a mouse anti-dengue virus type II monoclonal antibody, clone 3H5.1 (2.5 µg/ml; Merck Millipore) followed by an Alexa Fluor 488 goat anti-mouse antibody (4 µg/ml; Molecular Probes). Nuclei were stained with Hoechst 33342 (2 µg/ml; Molecular Probes). Fluorescent microscopic analysis was done with an Axiovert 200 M inverted microscope (Zeiss, Göttingen, Germany), using an EC Plan Apochromat 20x/0.8 objective.

## **3. Results**

### *3.1. Synthesis and purification of COOH-terminal peptides*

CXCL9 contains 103 amino acids and plays a key role in the trafficking of activated T cells and natural killer (NK) cells [53-55]. The COOH-terminal region of CXCL9 is remarkably long (residues 74 till 103) and basic (with 50 % positively charged amino acids) in comparison with other chemokines (Figure 1). Also CXCL12 $\gamma$ , a splicing variant of CXCL12, has a characteristic 30 amino acid long COOH-terminal tail (residues 68 till 98), containing 18 basic residues. Therefore, COOH-terminal peptides of CXCL9 and CXCL12 $\gamma$ , i.e. CXCL9(74-103), CXCL9(86-103), CXCL9(79-103), CXCL9(74-93), CXCL9(74-86), CXCL12 $\gamma$ (68-98) and CXCL12 $\gamma$ (77-98) were synthesized and purified by RP-HPLC. In addition, NH<sub>2</sub>-terminally acetylated and COOH-terminally amidated CXCL9(74-103) and NH<sub>2</sub>-terminally site-specifically biotinylated or fluorescently labeled CXCL9(74-103) and CXCL12 $\gamma$ (68-98) were

produced (Figure 1). Their Mr was confirmed by ion trap mass spectrometry as exemplified by CXCL12 $\gamma$ (68-98) and biotinylated CXCL12 $\gamma$ (68-98) (Figure 2).

### *3.2. Binding characteristics of COOH-terminal peptides to immobilized heparin*

Different viruses have been reported to use HSPGs as attachment/entry receptors on the surface of target cells. Therefore, compounds that competitively bind to HSPGs may block virus infection. To study the antiviral activity of the positively charged COOH-terminal CXCL9 and CXCL12 $\gamma$  peptides, the ability of the different peptides to bind heparin was first evaluated using surface plasmon resonance (SPR) analysis. Heparin was biotinylated as described in the materials and methods section and captured on immobilized neutravidin on a CM4 sensorchip. Kinetic analysis of the binding to heparin was performed by injecting increasing concentrations of the peptides over the heparin surface (Figure 3). The rising part of each curve (0-120 sec) corresponds to the association phase of the peptides to heparin, whereas the descending part (120-300 sec) represents the dissociation phase. The binding affinities ( $K_D$ ) were derived from steady state analysis using the Biacore T200 Evaluation Software (Table 1). These data indicate that the CXCL9(74-103) peptide binds to heparin with the highest affinity ( $K_D=3.1$  nM), whereas the acetyl-CXCL9(74-103)-amide peptide and CXCL9(74-93) bind with slightly lower but comparable affinity ( $K_D=8.8$  nM and  $K_D=11$  nM, respectively). This indicates that the ten COOH-terminal residues also play a role in the heparin binding affinity. In contrast, the CXCL9(79-103), CXCL9(86-103) and CXCL9(74-86) peptides showed lower or very weak affinity for heparin binding ( $K_D=162$  nM,  $K_D=820$  nM and  $K_D=3558$  nM, respectively), suggesting a major role for the GAG binding motif between Lys-85 and Lys-89 in CXCL9 for heparin binding. However, also the first GAG binding motif enhances the affinity for heparin. Both CXCL12 $\gamma$  derived peptides had high affinity for heparin.  $K_D$  values of 8 and 18 nM were calculated for CXCL12 $\gamma$ (68-98) and CXCL12 $\gamma$ (77-98), respectively.

### *3.3. Binding of CXCL9(74-103) and CXCL12 $\gamma$ (68-98) to cellular GAGs*

To determine the binding of the peptides to cellular GAGs, the two peptides with the lowest  $K_D$  on the heparin-coated sensorchips, i.e. CXCL9(74-103) and CXCL12 $\gamma$ (68-98), were site-specifically biotinylated at the NH<sub>2</sub>-terminus and binding of the biotinylated peptides to CHO cells was evaluated by flow cytometric analysis. To ensure that binding was GAG-mediated, CHO cells were treated with NaClO<sub>3</sub> to reduce the expression of cellular GAGs. Treatment of CHO cells resulted on average in 71.4 % reduction of HS expression, as an indication for the total GAG expression (data not shown). This reduction of HS expression is the result of the reduction in sulfation of HS. As seen in Figure 4A, CXCL12 $\gamma$ (68-98) bound dose-dependently to cellular GAGs on CHO cells. Remarkably, at lower concentrations, CXCL12 $\gamma$ (68-98) seemed to bind better to cellular GAGs than CXCL9(74-103), although it was not significant. Finally, treatment of the cells with NaClO<sub>3</sub> significantly reduced the binding of CXCL12 $\gamma$ (68-98) to cellular GAGs (Figure 4B).

#### *3.4. Antiviral activity of the COOH-terminal peptides*

The high affinities of the positively charged COOH-terminal peptides for heparin indicate that they may compete with endogenous and exogenous (e.g. viral) HSPG ligands for binding to immobilized heparin and cellular HSPGs. As such, these peptides may interfere with the attachment step during viral infection, since HS has been shown to serve as an attachment receptor for a number of viruses. Therefore, the antiviral capacity of the peptides was evaluated against 6 different human viruses that have been reported to use HSPGs for their attachment to target cells. CXCL9(74-103), acetyl-CXCL9(74-103)-amide, CXCL9(74-93) and both CXCL12 $\gamma$  peptides were found to exert antiviral activity against DENV-2 ( $EC_{50}$  values between 11 and 48  $\mu$ M), HSV-1 ( $EC_{50}$  values between 9 and 59  $\mu$ M) and RSV ( $EC_{50}$  values between 23  $\mu$ M to 115  $\mu$ M) (Table 2), without causing any cytotoxic effect ( $CC_{50} > 150$   $\mu$ M) (data not shown). The CXCL9(79-103) peptide was found to exert antiviral activity against HSV-1 ( $EC_{50} = 33.5$   $\mu$ M) and weakly against RSV ( $EC_{50} = 100$   $\mu$ M) and DENV-2 (no  $EC_{50}$  was reached). In general the CXCL9(74-103) peptide had the strongest antiviral activity, whereas CXCL9(86-103) and CXCL9(74-86) were unable to inhibit any of the viruses tested. The CXCL12 $\gamma$  peptides showed a 2- to 5-

fold lower antiviral activity against DENV-2, HSV-1 and RSV, when compared to CXCL9(74-103). No significant or a very weak (no EC<sub>50</sub> value reached at 100 µM) antiviral effect against HSV-2, VV and ADV-2 was observed for the peptides. In view of the striking difference in antiviral activity of the peptides against laboratory strains of HSV-1 and HSV-2, the antiviral activity of the peptides was tested against several clinical isolates of wild-type HSV-1 and HSV-2 from virus-infected individuals in Belgium. In these experiments the same trend was seen in that the peptides were more effective against HSV-1 compared to HSV-2 (Figure 5), suggesting that HSV-1 and HSV-2 attach to the host cells in a different way. Again, CXCL9(74-103) and acetyl-CXCL9(74-103)-amide peptides had the strongest antiviral activity, whereas CXCL9(86-103) and CXCL9(74-86) were unable to inhibit both HSV-1 and HSV-2 infection. Interestingly, dextran sulfate which also blocks attachment of the virus to the host cells was found to be more effective against HSV-2 than against HSV-1. This shows that there is indeed a difference in the infection of HEL cells with HSV-1 or HSV-2. No difference between anti-HSV-1 or anti-HSV-2 activity was seen for acyclovir, an antiviral which is used to treat HSV infections and targets the viral DNA polymerase [56]. To investigate whether the peptides could also bind directly to the virus thereby inducing virucidal activity, 100-fold concentrated HSV-1 was pre-incubated with 100 µM CXCL9(74-103). After 100-fold dilution (to obtain an inactive peptide but an active virus concentration) and subsequent infection of the cells, no antiviral effect of the peptides was seen (data not shown).

To further investigate the molecular details of anti-viral immunity from non-immune cells, including HEL, HeLa and HMEC-1 cells, cytokine levels of IL-6, TNF- $\alpha$ , IL-1 $\beta$ , IFN- $\alpha$  and IFN- $\beta$  were measured in the presence or absence of CXCL9(74-103) and CXCL9(86-103). No effect of the peptides was seen on either virus-induced or spontaneous cytokine production (data not shown). Next, the activation of caspase-1 was evaluated using the fluorescent caspase substrate Ac-YVAD-AMC. Also no direct effect of the peptides on caspase-1 activation was seen on non-infected HEL cells (Figure 6A), HeLa cells (Figure 6B) and HMEC-1 cells (Figure 6C). Further, the expression of HS on HEL and HeLa cells was determined by flow cytometric analysis, but no significant difference in HS expression was observed (Figure 6D). Therefore, it can be concluded that differences in antiviral activity against different viruses

(on other cell types) are not caused by a difference in HS expression, but more likely by the dependence of the particular virus on a specific GAG for infection.

### *3.5. The CXCL9(74-103) peptide competes with DENV envelope protein for binding to heparin*

Next, the anti-DENV activity of the CXCL9 or CXCL12 $\gamma$  peptides was studied in more detail. A dose-dependent inhibition of endothelial cell infection by DENV-2 was observed in the presence of increasing concentrations of the peptides (Figure 7A). CXCL9(74-103) showed the strongest anti-DENV activity with an EC<sub>50</sub> of 11  $\mu$ M, whereas the CXCL9(86-103) and CXCL9(74-86) peptide did not block the DENV infection of endothelial cells (EC<sub>50</sub> > 100  $\mu$ M). For the CXCL9(79-103) peptide some antiviral activity against DENV-2 was seen, but no EC<sub>50</sub> value could be calculated. The COOH-terminal CXCL12 $\gamma$  peptides could also inhibit DENV infection with an EC<sub>50</sub> of 22  $\mu$ M to 48  $\mu$ M. Next, the infectivity of DENV-2 in endothelial cells was visualized using immunocytochemistry (Figure 7B). This clearly showed that 20  $\mu$ M of fluorescently labeled CXCL9(74-103) binds to endothelial cells thereby inhibiting the infection by DENV-2. The DENV virion can attach to endothelial cells by the interaction of its envelope (E) protein with cell surface-associated HS-containing proteoglycans. Indeed, domain III of the E protein contains two putative GAG binding sites, which are assumed to be involved in the interaction between the DENV E protein and HSPGs. Since the COOH-terminal chemokine-derived peptide CXCL9(74-103) bound with high affinity to GAGs, the binding of DENV E domain III to heparin was investigated by SPR in the absence or presence of CXCL9(74-103) or the low affinity heparin-binding peptide CXCL9(86-103). The SPR sensorgrams show binding of DENV E domain III (E DIII) to captured heparin on a neutravidin CM4 chip in the presence (blue curve) or absence (red curves) of different concentrations of the CXCL9 peptides (Figure 8). Binding of the CXCL9-derived peptides in the absence of DENV E DIII is shown as a green line. When CXCL9(74-103) and DENV E DIII were applied at equimolar concentrations (400 nM) over the heparin surface, the binding curve coincides with that of the CXCL9(74-103) peptide alone, which suggests that DENV E DIII is unable to bind to heparin and only the CXCL9(74-103) peptide is bound (Figure 8A). Even when a ten-fold lower concentration of the

peptide (40 nM) is injected with DENV E DIII (400 nM), the peptide was still able to block the binding of DENV E DIII to heparin completely (Figure 8B). At a 100-fold molar excess of DENV E DIII (400 nM) over CXCL9(74-103) (4 nM), an increased resonance signal was measured when compared to binding of the peptide alone, which suggests binding of DENV E DIII to the immobilized heparin (Figure 8C). However, the binding curve at 4 nM CXCL9(74-103) plus DENV E DIII did not yet coincide with the curve of DENV E DIII in the absence of CXCL9(74-103), which indicates that the peptide is still able to partially block DENV E DIII binding. In contrast, CXCL9(86-103) could only moderately inhibit DENV E DIII binding when it was injected at equimolar concentrations (Figure 8D), whereas at 10-fold lower concentrations of CXCL9(86-103) the inhibition was completely abrogated (Figure 8E).

#### **4. Discussion**

In addition to their role in leukocyte migration during inflammation and infection, a number of chemokine ligands have been reported to have antibacterial, antifungal or parasiticidal activity independent of any interaction with their proper GPCRs [57-61]. One of the most potent chemoattractants with such direct antimicrobial activity is the CXC chemokine CXCL9 [58;62;63]. Upon infection, mononuclear cells, fibroblasts, endothelial and epithelial cells are stimulated by interferons to produce the CXC chemokine receptor 3 (CXCR3) ligands CXCL9, CXCL10 and CXCL11 [64;65]. Co-stimulation of these cells with interferons and microbial compounds such as toll-like receptor ligands may result in the production of large amounts of CXCL9 and CXCL10, i.e.  $\mu\text{g}$  levels of chemokine produced per  $10^6$  cells. CXCL9 and CXCL10 exert direct antibacterial effects that are comparable to the effects mediated by cationic antimicrobial peptides, like defensins [58]. The interferon-induced ligands for CXCR3 have also been reported to be important for the response to viral infections [66]. The importance of chemokines in antiviral defense is underscored by the existence of viral mimicry of the chemokine network including virally encoded seven transmembrane receptors which bind chemokines and allow viruses to escape from an efficient immune response [67]. CXCR3 is present on activated T cells and NK cells and therefore is an important receptor for the migration of these cells to sites of

infection. In general the effect of the CXCR3 ligands on lymphocyte and NK cell migration is thought to explain their crucial role in the antiviral response. CXCL9 is an exception in the chemokine family since it has a COOH-terminal sequence extension not present in other CXCR3 ligands but conserved across species. Recently, we observed that this COOH-terminal tail which contains mainly lysine residues is partially or completely removed from most of the natural CXCL9 proteins isolated from fibroblast or leukocyte cultures treated with inflammatory stimuli [44]. These COOH-terminally truncated CXCL9 proteins retain their CXCR3-dependent signaling properties *in vitro* [68]. Thus, the extended COOH-terminal sequence is not crucial for its GPCR-dependent signaling properties.

In addition to their interaction with GPCRs, chemokines are known to bind to heparin and other GAGs [22;40;41]. Although mutations in the chemokine GAG binding domains do not affect the interaction of chemokines with their specific GPCRs, these strongly reduce the *in vivo* chemotactic activity of chemokines [38;69;70]. In addition to CXCL9, CXCL12 $\gamma$ , a ligand for CXCR4, also has an extremely positively charged COOH-terminal tail not present in other chemokines. In this manuscript we demonstrate that peptides derived from the CXCL9 and CXCL12 $\gamma$  COOH-terminal sequences bind to GAGs with high affinity. GAGs on cellular HSPGs are not only present to prevent wash-out of chemokines on the endothelial layer of blood vessels but HSPGs are also used as (co-)receptor for attachment and/or entry by different viruses. Therefore, the interference with the viral attachment process is considered an attractive antiviral strategy [71;72]. Such antiviral compounds might be used to combat several unrelated viral infections. Also, it has been suggested that less resistance to such antivirals due to viral mutations can occur [2;8;33]. Many polyanions, as GAG mimicking agents, have been developed and evaluated to bind viruses, although the clinical use of these compounds has been limited because of the anticoagulant side-effects [72]. Alternatively, positively charged molecules that bind to cell surface-associated HSPGs may block viral attachment and infection [34]. Therefore, we evaluated the ability of several positively charged COOH-terminal chemokine-derived peptides to inhibit the replication of HSPG-binding viruses. We recently showed that intravenous injection of up to 100  $\mu$ g of such peptides in mice did not lead to toxicity [44]. The COOH-terminal peptides derived



from CXCL9 (30 amino acid-, 20 amino acid- and 18 amino acid-long) and CXCL12 $\gamma$  (31 amino acid- and 22 amino acid-long), which were tested in this study, have a pI of >11 and >12, respectively, comparable to the previously reported 20 amino acid-long synthetic anti-LPS peptides which also have a pI of >11 [33]. All chemokine-derived peptides tested in our study, with the exception of CXCL9(86-103) and CXCL9(74-86), bound with high affinity to immobilized heparin and cell-bound HS, which mimics GAGs on the target cells for HSPGs binding viruses. This could be explained by the presence of GAG binding motifs (BBXB and XBBBXXBX) in the peptides in which B is a positively charged amino acid. Indeed, CXCL9(74-103) and CXCL9(74-93) contain 2 typical GAG binding motifs between Lys-75 and Lys-78, and between Lys-85 and Lys-89, and were found to bind heparin with an affinity approximately 260-fold and 75-fold higher compared to CXCL9(86-103), which lacks the 2 GAG binding motifs. Although CXCL9(79-103) and CXCL9(74-86) contain 1 GAG binding motif (between Lys-85 and Lys-89 or Lys-75 and Lys-78, respectively), their affinity for heparin was found to be approximately 50-fold or 1200-fold lower compared to CXCL9(74-103). Two COOH-terminal CXCL12 $\gamma$  peptides tested in this study, i.e. CXCL12 $\gamma$ (68-98) and CXCL12 $\gamma$ (77-98), both containing 2 typical GAG binding motifs between Lys-77 and Lys-80, and between Lys-84 and Lys-88, displayed comparable heparin binding affinities which was reflected by the ability to inhibit viral infection. It seems that the presence of 2 GAG binding motifs is necessary for potent GAG interactions and the resulting antiviral activity. The low affinity of CXCL9(74-86) for heparin shows that not only the presence of GAG binding motifs, but also the length of the peptide is important. The CXCL9(74-93) peptide, which is only 7 amino acids longer than CXCL9(74-86), shows a much higher affinity for heparin. In addition, CXCL9(86-103) does not contain any consensus GAG binding motif but still shows 4-fold higher affinity for heparin than CXCL9(74-86). Except for CXCL9(86-103) and CXCL9(74-86), all tested COOH-terminal peptides exerted antiviral activity against RSV, HSV-1 and DENV-2 with EC<sub>50</sub> values ranging from 9  $\mu$ M to 115  $\mu$ M but were less or not active against HSV-2, VV, ADV-2. Although HS serves as an initial attachment site for both HSV-1 and HSV-2, remarkably less antiviral activity against HSV-2 was found. Even against different clinical isolates of HSV-1 and HSV-2, the same trend was observed. Such different antiviral activities are not

exceptional since even in the case of different serotypes of one HSV, specific recognition of different HS structures has been reported [73]. Also, differences in diversity, substitution rates and recombination rates between HSV-1 and HSV-2 glycoproteins were observed [74]. It can be suggested that HSV-2, ADV-2 and VV may use different GAGs as co-receptors for entering and infecting the host cells. If the peptides show lower affinity for the most important GAGs for a specific virus, one could presume that they have lower antiviral activity. Recently, it was already described that CXCL9(74-103) binds with high but different affinity to GAGs [44]. This specificity is mostly determined by the GAG binding motifs of the peptide. Another potential explanation for the difference in antiviral activity against these viruses is the importance of GAGs as co-receptors. It is possible that some viruses are more dependent on GAGs for infecting cells than others. Finally, anti-DENV-2 activity was further investigated and SPR analysis showed that CXCL9(74-103) was a very strong competitor for the binding of DENV E DIII to heparin.

In cell cultures, no toxic effect was detected with the chemokine-derived peptides up to concentrations of 150  $\mu$ M. In addition, no effect of the peptides on either spontaneous or virus-induced production of cytokines such as IFN- $\beta$  or on the activation of caspase-1 was observed. In view of this, the peptides derived from the natural COOH-terminal sequences of CXCL9 and CXCL12 $\gamma$  might be lead molecules for the generation of antiviral drugs that block the entry of viruses such as HSV-1, RSV and DENV-2 by binding to GAGs on target cells. The potency of these antiviral peptides may be increased by alternative formulations, as demonstrated for peptide-derived dendrimers [75-78]. As it is known that other viruses such as herpesviruses (e.g. cytomegalovirus, varicella-zoster virus, Epstein-barr virus), hepatitis viruses (e.g. HBV, HCV, HDV), HIV and human papillomavirus use HS as a (co-)receptor for entry, antiviral activity of the chemokine peptides could be tested against these viruses. Our observation also means that CXCL9 and CXCL12 $\gamma$  may not only be important for the antiviral response due to their chemoattractant properties for activated T cells and NK cells but in addition directly inhibit viral adsorption on the target cells in a chemokine receptor independent manner.

## **5. Acknowledgements**

The authors would like to thank Leentje Persoons, Eef Meyen, Sofie Knoops, Lotte Vanbrabant, Noémie Pörtner and Ellen De Waegenaere for excellent technical assistance. This research was supported by the Interuniversity Attraction Poles Programme initiated by the Belgian Science Policy Office (I.A.P. project 7/40), the Fund for Scientific Research of Flanders (FWO-Vlaanderen projects), the Concerted Research Actions of the Regional Government of Flanders (GOA/12/017) and the KU Leuven (PF no. 10/18). A.M. holds a postdoctoral research fellowship of the FWO-Vlaanderen. The Hercules foundation of the Flemish government provided funding to purchase LC-MS/MS equipment (contract AKUL/11/31). None of the sponsors had a role in the study design, the collection, analysis or interpretation of the data, in the writing of the report or in the decision to submit the article for publication.

## Reference List

1. De Clercq E. The design of drugs for HIV and HCV. *Nat Rev Drug Discov* 2007;6:1001-18.
2. Colman PM. New antivirals and drug resistance. *Annu Rev Biochem* 2009;78:95-118.
3. Henrich TJ and Kuritzkes DR. HIV-1 entry inhibitors: recent development and clinical use. *Curr Opin Virol* 2013;3:51-7.
4. Sulkowski MS, Kang M, Matining R, Wyles D, Johnson VA, Morse GD, et al. Safety and antiviral activity of the HCV entry inhibitor ITX5061 in treatment-naïve HCV-infected adults: a randomized, double-blind, phase 1b study. *J Infect Dis* 2014;209:658-67.
5. Qiu M, Chen Y, Song S, Song H, Chu Y, Yuan Z, et al. Poly (4-styrenesulfonic acid-co-maleic acid) is an entry inhibitor against both HIV-1 and HSV infections - potential as a dual functional microbicide. *Antiviral Res* 2012;96:138-47.
6. Lieberman-Blum SS, Fung HB, Bandres JC. Maraviroc: a CCR5-receptor antagonist for the treatment of HIV-1 infection. *Clin Ther* 2008;30:1228-50.
7. Van Der Ryst E. Maraviroc - A CCR5 Antagonist for the Treatment of HIV-1 Infection. *Front Immunol* 2015;6:277.
8. Alen MM, De Burghgraeve T, Kaptein SJ, Balzarini J, Neyts J, Schols D. Broad antiviral activity of carbohydrate-binding agents against the four serotypes of dengue virus in monocyte-derived dendritic cells. *PLoS One* 2011;6:e21658.
9. Costa VV, Fagundes CT, Souza DG, Teixeira MM. Inflammatory and innate immune responses in dengue infection: protection versus disease induction. *Am J Pathol* 2013;182:1950-61.
10. Spear PG, Shieh MT, Herold BC, WuDunn D, Koshy TI. Heparan sulfate glycosaminoglycans as primary cell surface receptors for herpes simplex virus. *Adv Exp Med Biol* 1992;313:341-53.
11. Shieh MT, WuDunn D, Montgomery RI, Esko JD, Spear PG. Cell surface receptors for herpes simplex virus are heparan sulfate proteoglycans. *J Cell Biol* 1992;116:1273-81.
12. Chen Y, Maguire T, Hileman RE, Fromm JR, Esko JD, Linhardt RJ, et al. Dengue virus infectivity depends on envelope protein binding to target cell heparan sulfate. *Nat Med* 1997;3:866-71.
13. Chung CS, Hsiao JC, Chang YS, Chang W. A27L protein mediates vaccinia virus interaction with cell surface heparan sulfate. *J Virol* 1998;72:1577-85.
14. Dehecchi MC, Tamanini A, Bonizzato A, Cabrini G. Heparan sulfate glycosaminoglycans are involved in adenovirus type 5 and 2-host cell interactions. *Virology* 2000;268:382-90.
15. Tyagi M, Rusnati M, Presta M, Giacca M. Internalization of HIV-1 tat requires cell surface heparan sulfate proteoglycans. *J Biol Chem* 2001;276:3254-61.
16. Leistner CM, Gruen-Bernhard S, Glebe D. Role of glycosaminoglycans for binding and infection of hepatitis B virus. *Cell Microbiol* 2008;10:122-33.

17. Alen MM and Schols D. Dengue virus entry as target for antiviral therapy. *J Trop Med* 2012;2012:628475.
18. Urban S, Bartenschlager R, Kubitz R, Zoulim F. Strategies to inhibit entry of HBV and HDV into hepatocytes. *Gastroenterology* 2014;147:48-64.
19. Tiwari V, Tarbutton MS, Shukla D. Diversity of heparan sulfate and HSV entry: basic understanding and treatment strategies. *Molecules* 2015;20:2707-27.
20. Gandhi NS and Mancera RL. The structure of glycosaminoglycans and their interactions with proteins. *Chem Biol Drug Des* 2008;72:455-82.
21. Faham S, Hileman RE, Fromm JR, Linhardt RJ, Rees DC. Heparin structure and interactions with basic fibroblast growth factor. *Science* 1996;271:1116-20.
22. Proudfoot AE. Chemokines and Glycosaminoglycans. *Front Immunol* 2015;6:246.
23. Rabenstein DL. Heparin and heparan sulfate: structure and function. *Nat Prod Rep* 2002;19:312-31.
24. Lindahl U and Li JP. Interactions between heparan sulfate and proteins-design and functional implications. *Int Rev Cell Mol Biol* 2009;276:105-59.
25. Lindahl U and Kjellen L. Pathophysiology of heparan sulphate: many diseases, few drugs. *J Intern Med* 2013;273:555-71.
26. Shukla D, Liu J, Blaiklock P, Shworak NW, Bai X, Esko JD, et al. A novel role for 3-O-sulfated heparan sulfate in herpes simplex virus 1 entry. *Cell* 1999;99:13-22.
27. Cladera J, Martin I, O'Shea P. The fusion domain of HIV gp41 interacts specifically with heparan sulfate on the T-lymphocyte cell surface. *EMBO J* 2001;20:19-26.
28. Shukla D and Spear PG. Herpesviruses and heparan sulfate: an intimate relationship in aid of viral entry. *J Clin Invest* 2001;108:503-10.
29. Herold BC, Gerber SI, Belval BJ, Siston AM, Shulman N. Differences in the susceptibility of herpes simplex virus types 1 and 2 to modified heparin compounds suggest serotype differences in viral entry. *J Virol* 1996;70:3461-9.
30. Feyzi E, Trybala E, Bergstrom T, Lindahl U, Spillmann D. Structural requirement of heparan sulfate for interaction with herpes simplex virus type 1 virions and isolated glycoprotein C. *J Biol Chem* 1997;272:24850-7.
31. O'Donnell CD, Kovacs M, Akhtar J, Valyi-Nagy T, Shukla D. Expanding the role of 3-O sulfated heparan sulfate in herpes simplex virus type-1 entry. *Virology* 2010;397:389-98.
32. Petcu DJ, Aldrich CE, Coates L, Taylor JM, Mason WS. Suramin inhibits in vitro infection by duck hepatitis B virus, Rous sarcoma virus, and hepatitis delta virus. *Virology* 1988;167:385-92.
33. Krepstakies M, Lucifora J, Nagel CH, Zeisel MB, Holstermann B, Hohenberg H, et al. A new class of synthetic peptide inhibitors blocks attachment and entry of human pathogenic viruses. *J Infect Dis* 2012;205:1654-64.

34. Dogra P, Martin EB, Williams A, Richardson RL, Foster JS, Hackenback N, et al. Novel heparan sulfate-binding peptides for blocking herpesvirus entry. *PLoS One* 2015;10:e0126239.
35. Baggiolini M, Dewald B, Moser B. Human chemokines: an update. *Annu Rev Immunol* 1997;15:675-705.
36. Murphy PM, Baggiolini M, Charo IF, Hebert CA, Horuk R, Matsushima K, et al. International union of pharmacology. XXII. Nomenclature for chemokine receptors. *Pharmacol Rev* 2000;52:145-76.
37. Murdoch C and Finn A. Chemokine receptors and their role in inflammation and infectious diseases. *Blood* 2000;95:3032-43.
38. Proudfoot AE, Handel TM, Johnson Z, Lau EK, LiWang P, Clark-Lewis I, et al. Glycosaminoglycan binding and oligomerization are essential for the in vivo activity of certain chemokines. *Proc Natl Acad Sci U S A* 2003;100:1885-90.
39. Rot A and von Andrian UH. Chemokines in innate and adaptive host defense: basic chemokines grammar for immune cells. *Annu Rev Immunol* 2004;22:891-928.
40. Handel TM, Johnson Z, Crown SE, Lau EK, Proudfoot AE. Regulation of protein function by glycosaminoglycans--as exemplified by chemokines. *Annu Rev Biochem* 2005;74:385-410.
41. Johnson Z, Proudfoot AE, Handel TM. Interaction of chemokines and glycosaminoglycans: a new twist in the regulation of chemokine function with opportunities for therapeutic intervention. *Cytokine Growth Factor Rev* 2005;16:625-36.
42. Raman D, Sobolik-Delmaire T, Richmond A. Chemokines in health and disease. *Exp Cell Res* 2011;317:575-89.
43. Zlotnik A and Yoshie O. The chemokine superfamily revisited. *Immunity* 2012;36:705-16.
44. Vanheule V, Janssens R, Boff D, Kitic N, Berghmans N, Ronsse I, et al. The positively charged COOH-terminal glycosaminoglycan binding CXCL9(74-103) peptide inhibits CXCL8-induced neutrophil extravasation and monosodium urate crystal-induced gout in mice. *J Biol Chem* 2015.
45. Laguri C, Sadir R, Rueda P, Baleux F, Gans P, Arenzana-Seisdedos F, et al. The novel CXCL12gamma isoform encodes an unstructured cationic domain which regulates bioactivity and interaction with both glycosaminoglycans and CXCR4. *PLoS One* 2007;2:e1110.
46. Ades EW, Candal FJ, Swerlick RA, George VG, Summers S, Bosse DC, et al. HMEC-1: establishment of an immortalized human microvascular endothelial cell line. *J Invest Dermatol* 1992;99:683-90.
47. Loos T, Mortier A, Proost P. Chapter 1. Isolation, identification, and production of posttranslationally modified chemokines. *Methods Enzymol* 2009;461:3-29.
48. Van Raemdonck K, Berghmans N, Vanheule V, Bugatti A, Proost P, Opendakker G, et al. Angiostatic, tumor inflammatory and anti-tumor effects of CXCL4(47-70) and CXCL4L1(47-70) in an EGF-dependent breast cancer model. *Oncotarget* 2014;5:10916-33.

49. Andrei G, Snoeck R, De Clercq E, Esnouf R, Fiten P, Opdenakker G. Resistance of herpes simplex virus type 1 against different phosphonylmethoxyalkyl derivatives of purines and pyrimidines due to specific mutations in the viral DNA polymerase gene. *J Gen Virol* 2000;81:639-48.
50. Andrei G, van den Oord J, Fiten P, Opdenakker G, De Wolf-Peeters C, De Clercq E, et al. Organotypic epithelial raft cultures as a model for evaluating compounds against alphaherpesviruses. *Antimicrob Agents Chemother* 2005;49:4671-80.
51. Sagi G, Otvos L, Ikeda S, Andrei G, Snoeck R, De Clercq E. Synthesis and antiviral activities of 8-alkynyl-, 8-alkenyl-, and 8-alkyl-2'-deoxyadenosine analogues. *J Med Chem* 1994;37:1307-11.
52. Vervaeke P, Alen M, Noppen S, Schols D, Oreste P, Liekens S. Sulfated Escherichia coli K5 polysaccharide derivatives inhibit dengue virus infection of human microvascular endothelial cells by interacting with the viral envelope protein E domain III. *PLoS One* 2013;8:e74035.
53. Loetscher M, Gerber B, Loetscher P, Jones SA, Piali L, Clark-Lewis I, et al. Chemokine receptor specific for IP10 and mig: structure, function, and expression in activated T-lymphocytes. *J Exp Med* 1996;184:963-9.
54. Groom JR and Luster AD. CXCR3 in T cell function. *Exp Cell Res* 2011;317:620-31.
55. Van Raemdonck K, Van den Steen PE, Liekens S, Van Damme J, Struyf S. CXCR3 ligands in disease and therapy. *Cytokine Growth Factor Rev* 2015;26:311-27.
56. De Clercq E, Andrei G, Snoeck R, De Bolle L, Naesens L, Degreve B, et al. Acyclic/carbocyclic guanosine analogues as anti-herpesvirus agents. *Nucleosides Nucleotides Nucleic Acids* 2001;20:271-85.
57. Yang D, Chen Q, Hoover DM, Staley P, Tucker KD, Lubkowski J, et al. Many chemokines including CCL20/MIP-3alpha display antimicrobial activity. *J Leukoc Biol* 2003;74:448-55.
58. Cole AM, Ganz T, Liese AM, Burdick MD, Liu L, Strieter RM. Cutting edge: IFN-inducible ELR-CXC chemokines display defensin-like antimicrobial activity. *J Immunol* 2001;167:623-7.
59. Crawford MA, Zhu Y, Green CS, Burdick MD, Sanz P, Alem F, et al. Antimicrobial effects of interferon-inducible CXC chemokines against Bacillus anthracis spores and bacilli. *Infect Immun* 2009;77:1664-78.
60. Karlsson C, Eliasson M, Olin AI, Morgelin M, Karlsson A, Malmsten M, et al. SufA of the opportunistic pathogen *finnegoldia magna* modulates actions of the antibacterial chemokine MIG/CXCL9, promoting bacterial survival during epithelial inflammation. *J Biol Chem* 2009;284:29499-508.
61. Sobirk SK, Morgelin M, Egesten A, Bates P, Shannon O, Collin M. Human chemokines as antimicrobial peptides with direct parasitocidal effect on *Leishmania mexicana* in vitro. *PLoS One* 2013;8:e58129.
62. Egesten A, Eliasson M, Johansson HM, Olin AI, Morgelin M, Mueller A, et al. The CXC chemokine MIG/CXCL9 is important in innate immunity against *Streptococcus pyogenes*. *J Infect Dis* 2007;195:684-93.

63. Reid-Yu SA, Tuinema BR, Small CN, Xing L, Coombes BK. CXCL9 contributes to antimicrobial protection of the gut during citrobacter rodentium infection independent of chemokine-receptor signaling. *PLoS Pathog* 2015;11:e1004648.
64. Proost P, Verpoest S, Van de Borne K, Schutyser E, Struyf S, Put W, et al. Synergistic induction of CXCL9 and CXCL11 by Toll-like receptor ligands and interferon-gamma in fibroblasts correlates with elevated levels of CXCR3 ligands in septic arthritis synovial fluids. *J Leukoc Biol* 2004;75:777-84.
65. Loos T, Dekeyzer L, Struyf S, Schutyser E, Gijssbers K, Gouwy M, et al. TLR ligands and cytokines induce CXCR3 ligands in endothelial cells: enhanced CXCL9 in autoimmune arthritis. *Lab Invest* 2006;86:902-16.
66. Mahalingam S, Foster PS, Lobigs M, Farber JM, Karupiah G, Interferon-inducible chemokines and immunity to poxvirus infections. *Immunol Rev* 2000;177:127-33.
67. Rosenkilde MM, Smit MJ, Waldhoer M. Structure, function and physiological consequences of virally encoded chemokine seven transmembrane receptors. *Br J Pharmacol* 2008;153 Suppl 1:S154-S166.
68. Clark-Lewis I, Mattioli I, Gong JH, Loetscher P. Structure-function relationship between the human chemokine receptor CXCR3 and its ligands. *J Biol Chem* 2003;278:289-95.
69. Campanella GS, Grimm J, Manice LA, Colvin RA, Medoff BD, Wojtkiewicz GR, et al. Oligomerization of CXCL10 is necessary for endothelial cell presentation and in vivo activity. *J Immunol* 2006;177:6991-8.
70. Severin IC, Gaudry JP, Johnson Z, Kungl A, Jansma A, Gesslbauer B, et al. Characterization of the chemokine CXCL11-heparin interaction suggests two different affinities for glycosaminoglycans. *J Biol Chem* 2010;285:17713-24.
71. Liu J and Thorp SC. Cell surface heparan sulfate and its roles in assisting viral infections. *Med Res Rev* 2002;22:1-25.
72. Rusnati M, Vicenzi E, Donalisio M, Oreste P, Landolfo S, Lembo D. Sulfated K5 Escherichia coli polysaccharide derivatives: A novel class of candidate antiviral microbicides. *Pharmacol Ther* 2009;123:310-22.
73. Herold BC, Gerber SI, Belval BJ, Siston AM, Shulman N. Differences in the susceptibility of herpes simplex virus types 1 and 2 to modified heparin compounds suggest serotype differences in viral entry. *J Virol* 1996;70:3461-9.
74. Lamers SL, Newman RM, Laeyendecker O, Tobian AA, Colgrove RC, Ray SC, et al. Global Diversity within and between Human Herpesvirus 1 and 2 Glycoproteins. *J Virol* 2015;89:8206-18.
75. Luganini A, Giuliani A, Pirri G, Pizzuto L, Landolfo S, Gribaudo G. Peptide-derivatized dendrimers inhibit human cytomegalovirus infection by blocking virus binding to cell surface heparan sulfate. *Antiviral Res* 2010;85:532-40.
76. Donalisio M, Rusnati M, Civra A, Bugatti A, Allemand D, Pirri G, et al. Identification of a dendrimeric heparan sulfate-binding peptide that inhibits infectivity of genital types of human papillomaviruses. *Antimicrob Agents Chemother* 2010;54:4290-9.



77. Lugini A, Nicoletto SF, Pizzuto L, Pirri G, Giuliani A, Landolfo S, et al. Inhibition of herpes simplex virus type 1 and type 2 infections by peptide-derivatized dendrimers. *Antimicrob Agents Chemother* 2011;55:3231-9.
78. Donalio M, Rusnati M, Cagno V, Civra A, Bugatti A, Giuliani A, et al. Inhibition of human respiratory syncytial virus infectivity by a dendrimeric heparan sulfate-binding peptide. *Antimicrob Agents Chemother* 2012;56:5278-88.

**Table 1. Affinity data of the binding of CXCL9 and CXCL12 $\gamma$  peptides to heparin**

<b>COOH-terminal peptide</b>	<b>K<sub>D</sub> (nM) <sup>A</sup></b>
CXCL9(74-103)	3.1 ± 1.3
Acetyl-CXCL9(74-103)-amide	8.8 ± 5.0
CXCL9(86-103)	820 ± 240
CXCL9(79-103)	162 ± 23
CXCL9(74-93)	11 ± 4.8
CXCL9(74-86)	3558 ± 792
CXCL12 $\gamma$ (68-98)	8.0 ± 0.3
CXCL12 $\gamma$ (77-98)	18 ± 1.5

<sup>A</sup>Data are the mean ( $\pm$ SD) of at least three independent experiments. K<sub>D</sub>: binding affinity was calculated from steady state analysis

**Table 2. Antiviral activity of the COOH-terminal peptides**

COOH-terminal peptide	EC <sub>50</sub> <sup>A</sup> (μM)					
	ADV-2	DENV-2	HSV-1	HSV-2	RSV	VV
CXCL9(74-103)	>100	11 ± 4	15 ± 10	>100	23 ± 0	>100
Acetyl-CXCL9(74-103)-amide	>100	21 ± 4	9 ± 7	>100	31 ± 11	>100
CXCL9(86-103)	>100	>100	>100	>100	>100	>100
CXCL9(79-103)	>100	>100	33.5 ± 9	>100	100	>100
CXCL9(74-93)	>100	43 ± 13	14 ± 14	>100	50 ± 1	>100
CXCL9(74-86)	>100	>100	>100	>100	>100	>100
CXCL12γ(68-98)	>100	22 ± 3	39 ± 14	>100	115 ± 2	>100
CXCL12γ(77-98)	>100	48 ± 21	59 ± 15	>100	109 ± 12	>100

<sup>A</sup> 50 % effective concentration, required to reduce virus-infected cytopathogenicity or the number of infected cells by 50 %. Data shown are the mean (± SD) of three independent experiments. ADV: adenovirus, DENV: dengue virus, HSV-1: herpes simplex virus type 1 (KOS strain), HSV-2: herpes simplex virus type 2 (G strain), RSV: respiratory syncytial virus, VV: vaccinia virus

Peptide	Amino acid sequence	pI (theor.)	Mr (theor.)	Mr (exp.)
CXCL9(74-103)	<u>74</u> <u>K</u> <u>K</u> <u>K</u> <u>Q</u> <u>K</u> <u>N</u> <u>G</u> <u>K</u> <u>K</u> <u>H</u> <u>Q</u> <u>K</u> <u>K</u> <u>V</u> <u>L</u> <u>K</u> <u>V</u> <u>R</u> <u>K</u> <u>S</u> <u>Q</u> <u>R</u> <u>S</u> <u>R</u> <u>Q</u> <u>K</u> <u>K</u> <u>T</u> <u>T</u> <u>103</u>	12.34	3661.4	3661.2
Acetyl-CXCL9(74-103)-amide	<u>74</u> <u>K</u> <u>K</u> <u>Q</u> <u>K</u> <u>N</u> <u>G</u> <u>K</u> <u>K</u> <u>H</u> <u>Q</u> <u>K</u> <u>K</u> <u>V</u> <u>L</u> <u>K</u> <u>V</u> <u>R</u> <u>K</u> <u>S</u> <u>Q</u> <u>R</u> <u>S</u> <u>R</u> <u>Q</u> <u>K</u> <u>K</u> <u>T</u> <u>T</u> <u>103</u> *	<i>N.D.</i>	3702.5	3703.0
CXCL9(86-103)	<u>86</u> <u>K</u> <u>K</u> <u>V</u> <u>L</u> <u>K</u> <u>V</u> <u>R</u> <u>K</u> <u>S</u> <u>Q</u> <u>R</u> <u>S</u> <u>R</u> <u>Q</u> <u>K</u> <u>K</u> <u>T</u> <u>T</u> <u>103</u>	12.32	2199.7	2199.8
CXCL9(79-103)	<u>79</u> <u>N</u> <u>G</u> <u>K</u> <u>K</u> <u>H</u> <u>Q</u> <u>K</u> <u>K</u> <u>V</u> <u>L</u> <u>K</u> <u>V</u> <u>R</u> <u>K</u> <u>S</u> <u>Q</u> <u>R</u> <u>S</u> <u>R</u> <u>Q</u> <u>K</u> <u>K</u> <u>T</u> <u>T</u> <u>103</u>	12.33	3020.6	3020.8
CXCL9(74-93)	<u>74</u> <u>K</u> <u>K</u> <u>Q</u> <u>K</u> <u>N</u> <u>G</u> <u>K</u> <u>K</u> <u>H</u> <u>Q</u> <u>K</u> <u>K</u> <u>V</u> <u>L</u> <u>K</u> <u>V</u> <u>R</u> <u>K</u> <u>93</u>	11.59	2460.1	2458.8
CXCL9(74-86)	<u>74</u> <u>K</u> <u>K</u> <u>Q</u> <u>K</u> <u>N</u> <u>G</u> <u>K</u> <u>K</u> <u>H</u> <u>Q</u> <u>K</u> <u>86</u>	10.85	1607.9	1606.5
CXCL12γ(68-98)	<u>68</u> <u>K</u> <u>G</u> <u>R</u> <u>R</u> <u>E</u> <u>E</u> <u>K</u> <u>V</u> <u>G</u> <u>K</u> <u>E</u> <u>K</u> <u>I</u> <u>G</u> <u>K</u> <u>K</u> <u>R</u> <u>Q</u> <u>K</u> <u>K</u> <u>R</u> <u>K</u> <u>R</u> <u>K</u> <u>A</u> <u>A</u> <u>Q</u> <u>K</u> <u>R</u> <u>K</u> <u>N</u> <u>98</u>	11.57	3748.5	3748.6
CXCL12γ(77-98)	<u>77</u> <u>K</u> <u>K</u> <u>E</u> <u>I</u> <u>G</u> <u>K</u> <u>K</u> <u>R</u> <u>Q</u> <u>K</u> <u>K</u> <u>R</u> <u>K</u> <u>A</u> <u>A</u> <u>Q</u> <u>K</u> <u>R</u> <u>K</u> <u>N</u> <u>98</u>	11.81	2708.3	2708.1
Biotinylated CXCL9(74-103)	Biotin- <u>74</u> <u>K</u> <u>K</u> <u>Q</u> <u>K</u> <u>N</u> <u>G</u> <u>K</u> <u>K</u> <u>H</u> <u>Q</u> <u>K</u> <u>K</u> <u>V</u> <u>L</u> <u>K</u> <u>V</u> <u>R</u> <u>K</u> <u>S</u> <u>Q</u> <u>R</u> <u>S</u> <u>R</u> <u>Q</u> <u>K</u> <u>K</u> <u>T</u> <u>T</u> <u>103</u>	<i>N.D.</i>	3887.7	3890.5
Biotinylated CXCL12γ(68-98)	Biotin- <u>68</u> <u>K</u> <u>G</u> <u>R</u> <u>R</u> <u>E</u> <u>E</u> <u>K</u> <u>V</u> <u>G</u> <u>K</u> <u>E</u> <u>K</u> <u>I</u> <u>G</u> <u>K</u> <u>K</u> <u>R</u> <u>Q</u> <u>K</u> <u>K</u> <u>R</u> <u>K</u> <u>R</u> <u>K</u> <u>A</u> <u>A</u> <u>Q</u> <u>K</u> <u>R</u> <u>K</u> <u>N</u> <u>98</u>	<i>N.D.</i>	3974.8	3974.1
TAMRA-labeled CXCL9(74-103)	TAMRA- <u>74</u> <u>K</u> <u>K</u> <u>Q</u> <u>K</u> <u>N</u> <u>G</u> <u>K</u> <u>K</u> <u>H</u> <u>Q</u> <u>K</u> <u>K</u> <u>V</u> <u>L</u> <u>K</u> <u>V</u> <u>R</u> <u>K</u> <u>S</u> <u>Q</u> <u>R</u> <u>S</u> <u>R</u> <u>Q</u> <u>K</u> <u>K</u> <u>T</u> <u>T</u> <u>103</u>	<i>N.D.</i>	4073.9	4074.3

**Figure 1. Overview of the synthesized COOH-terminal peptides of CXCL9 and CXCL12γ**

The theoretical pI, Mr and experimentally determined Mr are listed. For clarity, basic amino acids were underlined. *N.D.*: not determined (\*\* NH<sub>2</sub>-terminally acetylated \* COOH-terminally amidated)

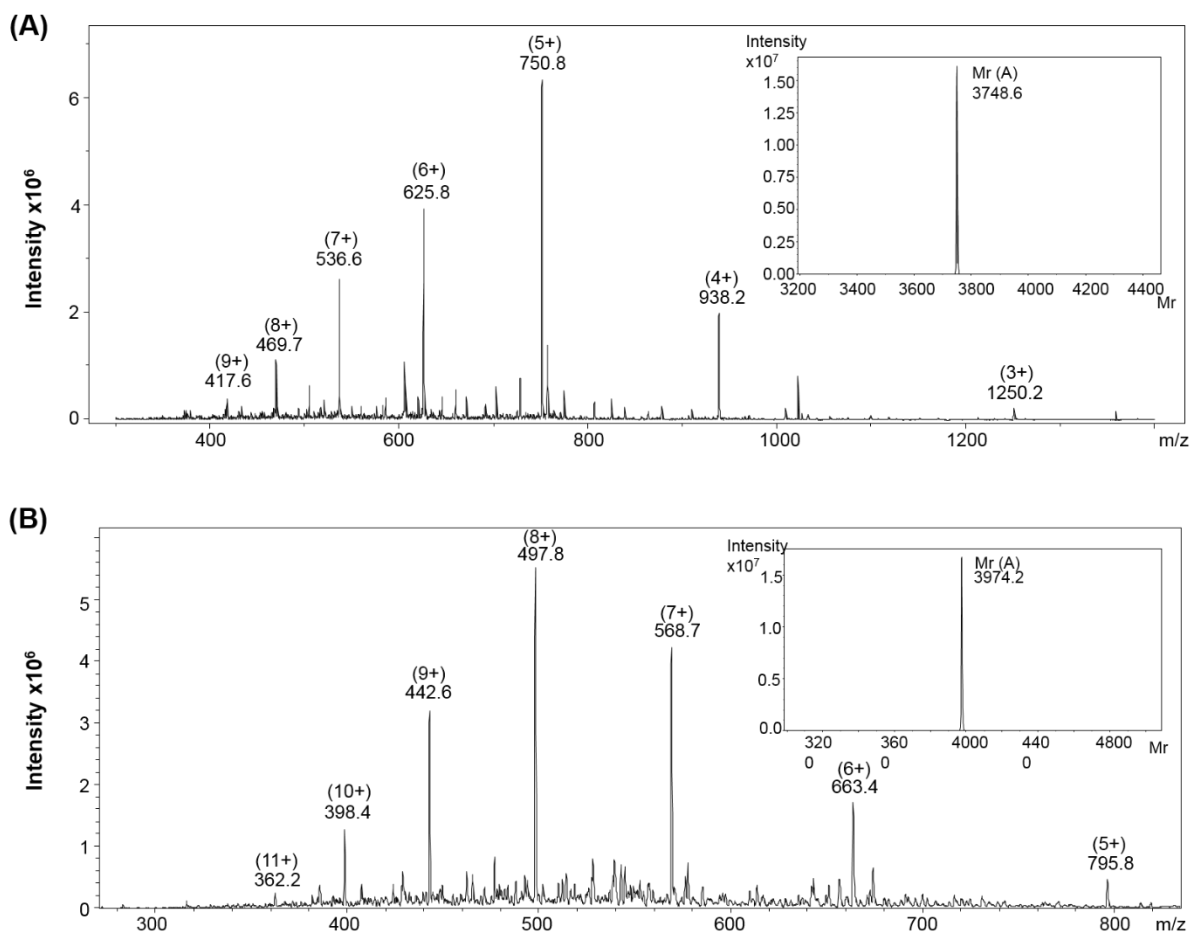


**Figure 2. Synthesis of COOH-terminal peptides of CXCL12 $\gamma$**

The chemokine-derived COOH-terminal peptides CXCL12 $\gamma$ (68-98) and NH<sub>2</sub>-terminally site-specifically biotinylated CXCL12 $\gamma$ (68-98) were chemically synthesized based on Fmoc-chemistry. The averaged mass spectra of purified CXCL12 $\gamma$ (68-98) [panel A] and biotinylated CXCL12 $\gamma$ (68-98) [panel B] are shown. The deconvoluted experimentally determined mass spectra indicating the Mr of the COOH-terminal CXCL12 $\gamma$  peptides are shown as inserts on the upper right of the averaged mass spectra.

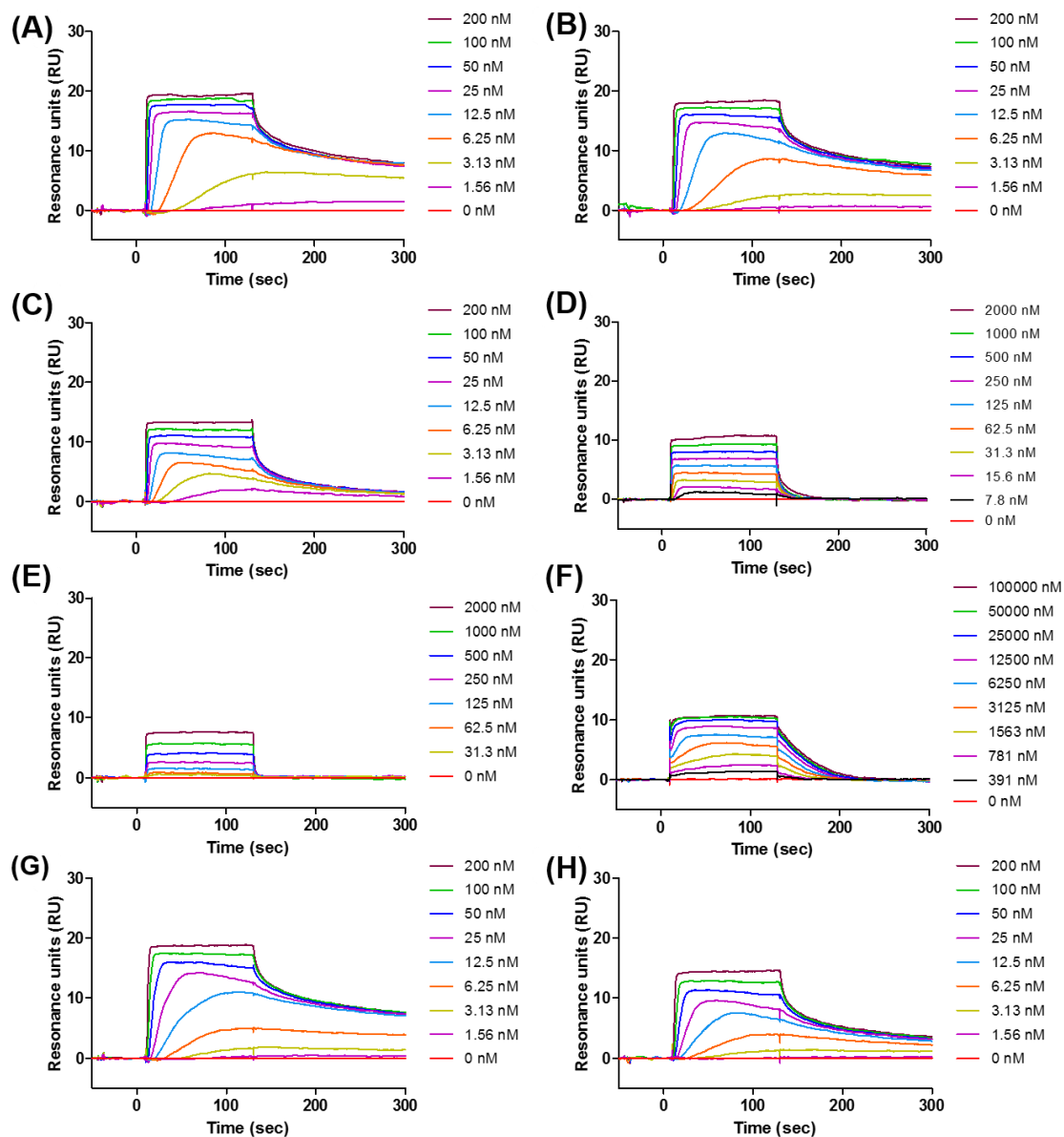


**Figure 3. Surface plasmon resonance (SPR) analysis of the interaction between COOH-terminal peptides of CXCL9 and CXCL12 $\gamma$  and heparin.**

Sensorgrams show the binding of different concentrations of CXCL9(74-103) [A], acetyl-CXCL9(74-103)-amide [B], CXCL9(74-93) [C], CXCL9(79-103) [D], CXCL9(86-103) [E], CXCL9(74-86) [F], CXCL12 $\gamma$ (68-98) [G] and CXCL12 $\gamma$ (77-98) [H] to immobilized heparin. The binding curves of 0 to 120 sec show the association, whereas those of 120 to 300 sec show the dissociation phase. The y-axis indicates the resonance signal as shown in resonance units (RU). The SPR analysis of one typical experiment is shown.

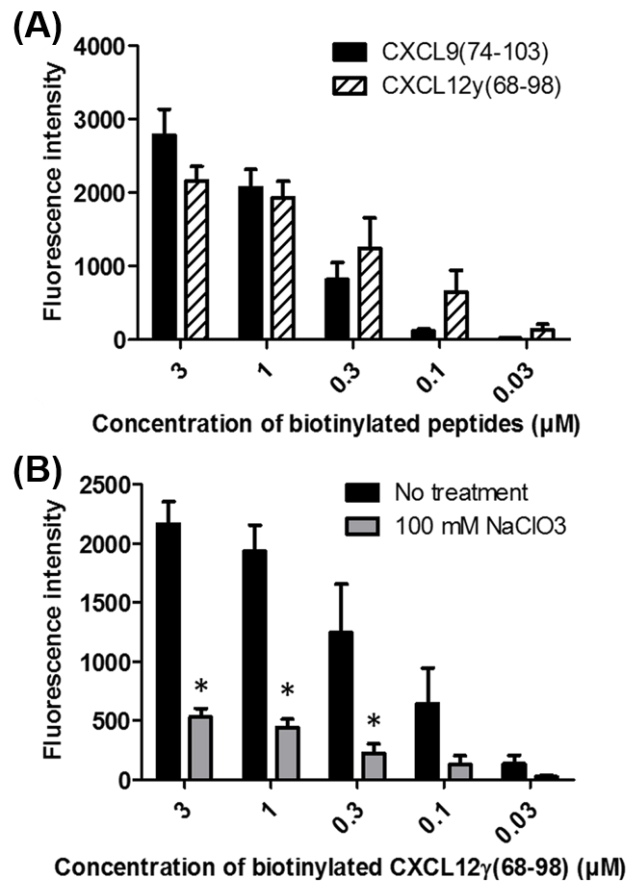


**Figure 4. Binding of COOH-terminal peptides to cellular GAGs**

Dose-dependent binding of NH<sub>2</sub>-terminally biotinylated CXCL9(74-103) and CXCL12 $\gamma$ (68-98) to CHO cells was assessed by flow cytometric analysis (panel A). The y-axis shows the fluorescence intensity of streptavidin-allophycocyanin. Panel B shows the binding of biotinylated CXCL12 $\gamma$ (68-98) to CHO cells treated or not treated with sodium chlorate (NaClO<sub>3</sub>). Treatment with NaClO<sub>3</sub> reduces the expression of GAGs so that binding of the COOH-terminal peptides was ensured to be GAG-mediated. Statistical comparison to evaluate the binding of biotinylated peptides on cells treated or not treated with NaClO<sub>3</sub> was performed using the Mann-Whitney U-test [n=6; \* p < 0.05].

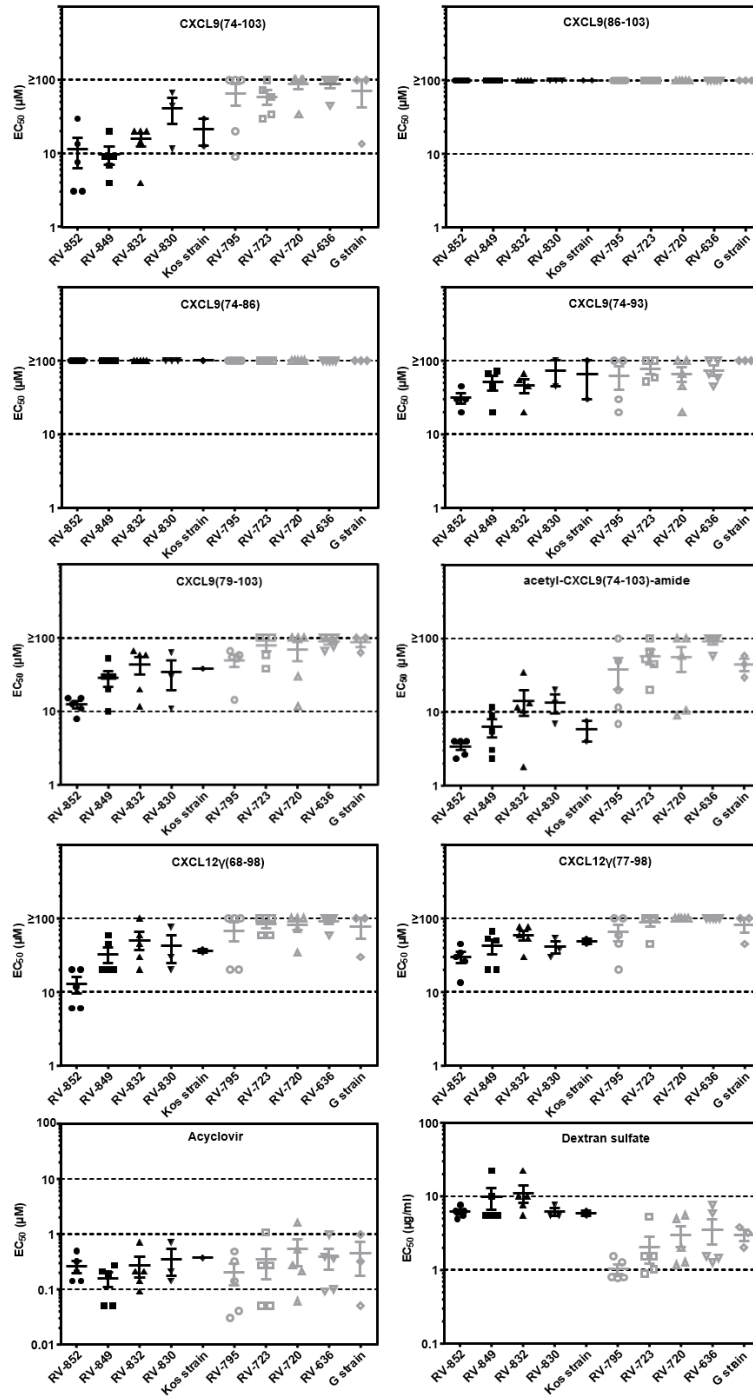


**Figure 5. Antiviral activity of the COOH-terminal peptides against clinical isolates of HSV-1 and HSV-2**

Antiviral activity against HSV-1 KOS strain, HSV-2 G strain and clinical isolates of wild-type HSV-1 (RV-852, RV-849, RV-832, RV-830) and HSV-2 (RV-795, RV-723, RV-720, RV-636) were determined on HEL cells. The  $EC_{50}$  values of at least three independent experiments are shown together with the mean ( $\pm$  SEM).



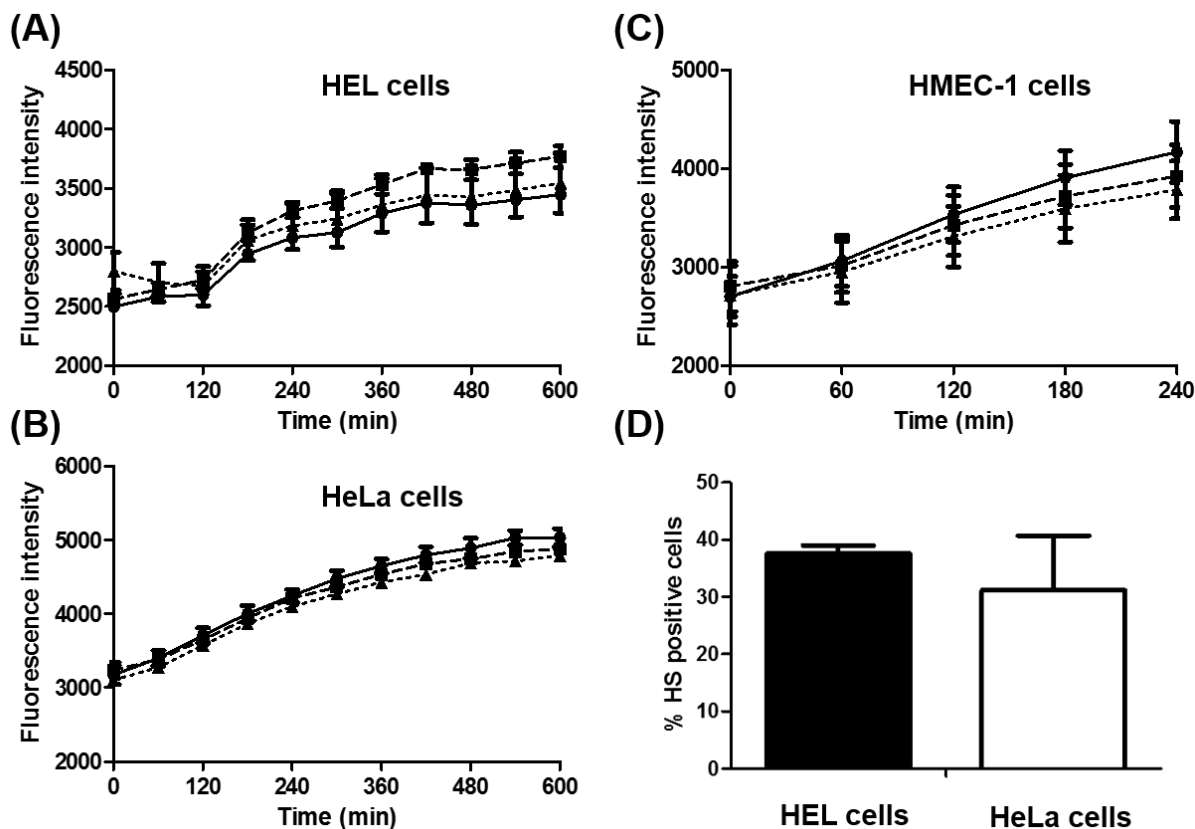


**Figure 6. Effect of the COOH-terminal peptides on the activation of caspase-1 and evaluation of the expression of heparan sulfate (HS) in HEL and HeLa cells**

The activation of caspase-1 was determined in HEL (A), HeLa (B) and HMEC-1 cells (C). Therefore cells, treated with vehicle [filled circles], 25  $\mu$ M CXCL9(74-103) [filled square) or CXCL9(86-103) [filled triangles], were lysed and incubated with the caspase-1 substrate Ac-YVAD-AMC. Fluorescence intensity was measured for 4 h (C) or 10 h (A, B) to visualize caspase-1-dependent Ac-YVAD-AMC cleavage. Data originate from one representative experiment out of two and are the mean ( $\pm$  SEM) of the fluorescence intensity of 3 independent cell lysates. Panel D shows the expression of HS on HEL and HeLa cells as assessed by staining cells with a specific mouse monoclonal anti-human HS antibody and a secondary PE-labeled goat anti-mouse antibody.

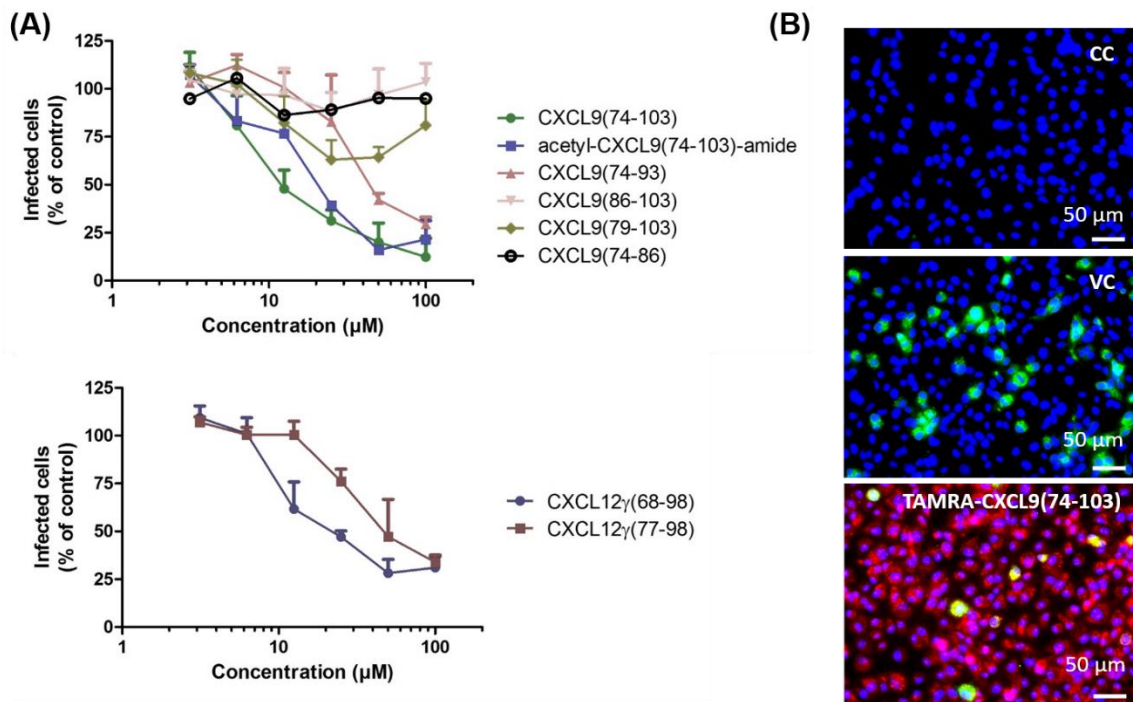


**Figure 7. Dose-dependent anti-DENV-2 activity of CXCL9 or CXCL12 $\gamma$  peptides in endothelial cells and immunofluorescent staining of DENV-2**

HMEC-1 cells were infected with DENV-2 in the presence of different concentrations of CXCL9 (panel A, upper) or CXCL12 $\gamma$  peptides (panel A, lower). Viral infectivity was quantified 24 h after infection by flow cytometry using an anti-DENV-2 specific antibody. Data represent the percentage of infected cells relative to the virus control. The mean (+ SD) of three independent experiments is shown (panel A). Panel B shows immunofluorescent staining of DENV-2 attachment to HMEC-1 cells. HMEC-1 cells were incubated with DENV-2 in the presence or absence of 20  $\mu\text{M}$  TAMRA-labeled CXCL9(74-103). Next, the nuclei (blue) and DENV-2 particles (green) were stained with Hoechst 33342 or a mouse anti-dengue virus type II monoclonal antibody, respectively. CC: cell control without virus, VC: virus control without TAMRA-labeled CXCL9(74-103)

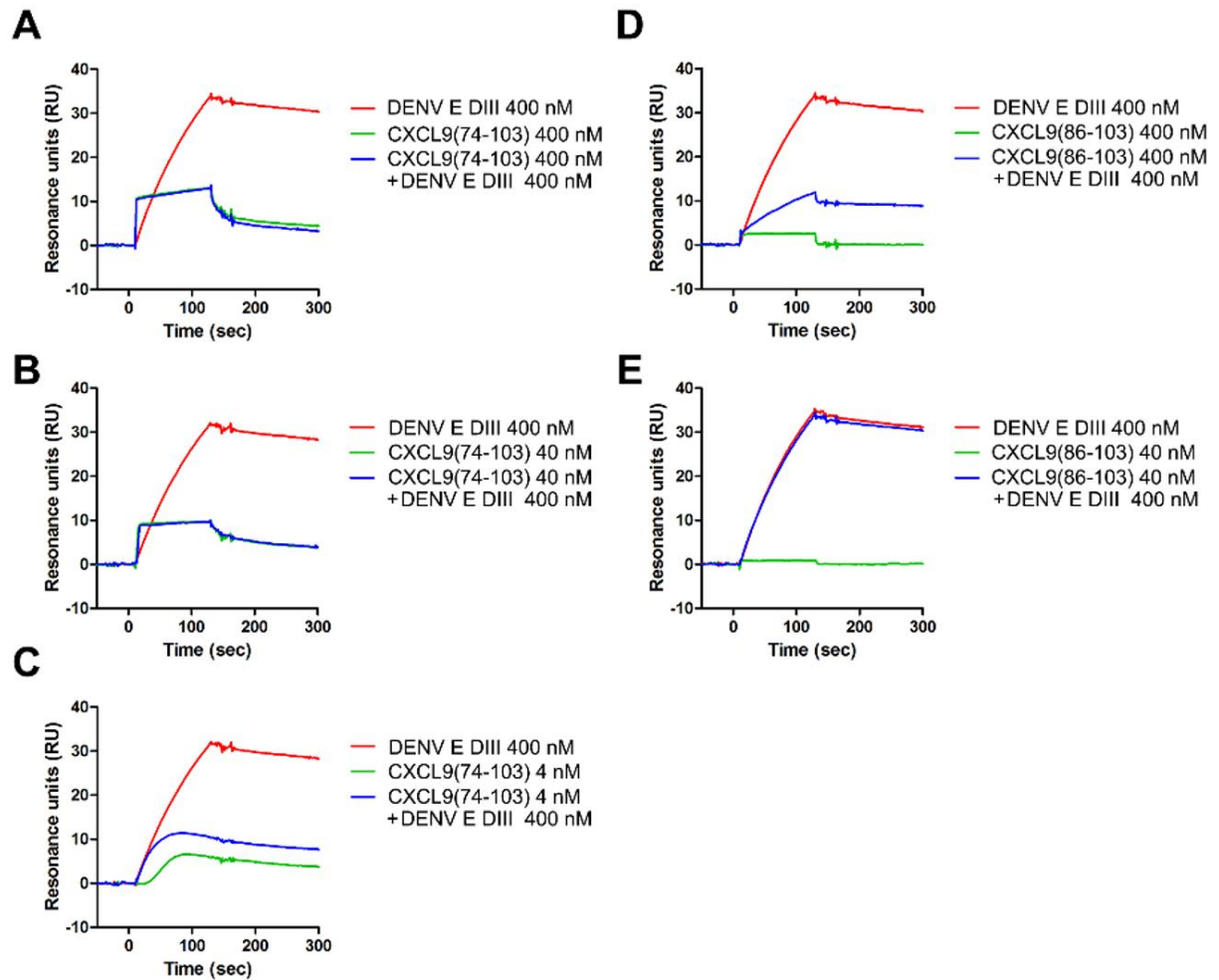


**Figure 8. Surface plasmon resonance (SPR) analysis of the competition between CXCL9 peptides and DENV E domain III for binding to heparin**

Sensorgrams show the binding of DENV envelope protein domain III (E DIII) to heparin in the presence (blue) or absence (red) of different concentrations of the CXCL9(74-103) (A-C) and CXCL9(86-103) (D, E) peptides. The binding of CXCL9 peptides in the absence of DENV E DIII is shown in green. The binding curves of 0 to 120 sec show the association, whereas those of 120 to 300 sec show the dissociation phase. The y-axis indicates the resonance signal as shown in resonance units (RU).